Thermal Vaporization of Biological Nanoparticles: Fragment-Free Vacuum Ultraviolet Photoionization Mass Spectra of Tryptophan, Phenylalanine−Glycine−Glycine, and β-Carotene

Kevin R. Wilson,[†] Michael Jimenez-Cruz,[†] Christophe Nicolas,[†] Leonid Belau,[†] Stephen R. Leone,[†,‡] and Musahid Ahmed*[,†]

Chemical Sciences Division, Lawrence Berkeley National Laboratory, and Departments of Chemistry and Physics, University of California, Berkeley, California 94720

Received: August 5, 2005; In Final Form: November 7, 2005

A simple, new way to introduce fragile biomolecules into the gas phase via thermal vaporization of nanoparticles is described. The general utility of this technique for the study of biomolecules is demonstrated by coupling this source to tunable synchrotron vacuum ultraviolet radiation. Fragment-free photoionization mass spectra of tryptophan, phenylalanine−glycine−glycine, and β-carotene are detected with signal-to-noise ratios exceeding 100. The 8.0 eV photoionization mass spectrum of tryptophan nanoparticles vaporized at 373 K is dominated by a single parent ion peak that exhibits a 20-fold enhancement over the methylene indole fragment ion. The degree of dissociative photoionization of tryptophan can be precisely controlled either by the thermal energy imparted into the neutral tryptophan molecule or by the energy of the ionizing photon. The results reveal how ∼0.5 eV changes in internal energy affect both the photoionization mass spectrum of tryptophan and the appearance energy of the daughter ion fragments. This method allows the ionization energies of glycine (9.3 ± 0.1 eV), tryptophan (7.3 ± 0.2 eV), phenylalanine (8.6 ± 0.1 eV), phenylalanine−glycine−glycine (9.1 ± 0.1 eV), and β-carotene (<7.0 eV) molecules to be determined directly from the photoionization efficiency spectra.

Introduction

Electrospray ionization (ESI) and matrix-assisted laser desorption (MALDI) methods have revolutionized the study of proteins and are now indispensable analytical tools in the modern molecular biology laboratory.[1] As a result, there is much interest in developing new techniques to obtain "fragment-free" mass spectra of fragile biomolecules such as amino acids, polypeptides, proteins, and DNA. These techniques are not only useful analytical tools for proteomics[2] but are essential for measuring fundamental electronic properties of bare biomolecules in the absence of solvent.[3] The ability to introduce significant quantities of intact *neutral* biomolecules into the gas phase is the only means for conducting fundamental investigations of conformational and structural dynamics of amino acids, polypeptides, and DNA bases by various spectroscopic methods, including photoelectron[4] and UV−IR double resonant spectroscopies.[5] Furthermore, fundamental electronic properties of many important biomolecules, such as ionization energies, proton and electron affinities, and dipole moments, are not known and can only be measured if these molecules can be successfully transported intact into the gas phase.

The occurrence of fragmentation in a mass spectrum is extremely sensitive to the amount of internal vibrational or rotational energy within the parent ion or neutral molecule.[6] This has led to the development of "soft" ionization techniques that deposit minimal amounts of internal energy into the molecule during ionization. For biomolecules, there is often another and perhaps even more important contributor to internal energy (and therefore the occurrence of fragmentation in mass spectra)— that is, the internal energy imparted to the neutral molecule in order to introduce it into the gas phase. This is because many amino acids, polypeptides, and most proteins have low vapor pressures and easily decompose at elevated temperatures. As a result, vibrationally "hot" molecules are unwanted byproducts of the high-temperature laser desorption or ablation techniques commonly employed to introduce large quantities of molecules into the gas phase for mass spectrometry analysis. To reduce the dissociative ionization of these vibrationally excited molecules, jet cooling in a supersonic molecular beam is generally necessary to recover appreciable intensity of the parent ion in the mass spectrum.[7]

Here we report a new method to introduce amino acids and polypeptides into the gas phase via formation of aerosol nanoparticles, followed by thermal vaporization and detection by tunable vacuum ultraviolet (VUV) photoionization mass spectrometry. The general strategy is to synthesize dry nanoparticles comprised of amino acids or polypeptides that are then thermally vaporized in high vacuum. The resulting vapor, containing neutral biomolecules, can be "softly" ionized with tunable VUV synchrotron radiation, producing nearly fragmentation-free mass spectra. In fact, the degree of fragmentation can be finely controlled via the thermal or photon energy, yielding greater insight into the role of internal energy in the photoionization mass spectra of amino acids and other biomolecules.

To first demonstrate the general utility of this approach and to illustrate how internal energy affects single photon ionization mass spectra, we examine the amino acids tryptophan, glycine,

* To whom correspondence should be addressed. Phone: (510) 486-6355. Fax: (510) 486-5311. E-mail: mahmed@lbl.gov.
† Chemical Sciences Division, Lawrence Berkeley National Laboratory.
‡ Departments of Chemistry and Physics.

10.1021/jp0543734 CCC: $33.50
Published on Web 12/18/2005

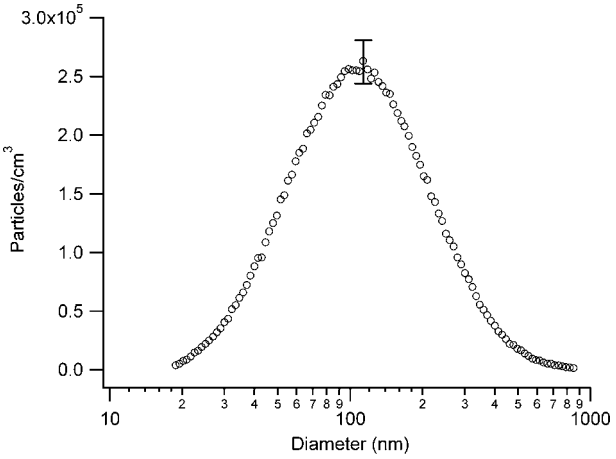

Figure 1. Particle size distribution of tryptophan obtained by atomizing a 1 g/L aqueous solution. The error bar shows the average fluctuation of the aerosol source over a 12 h period.

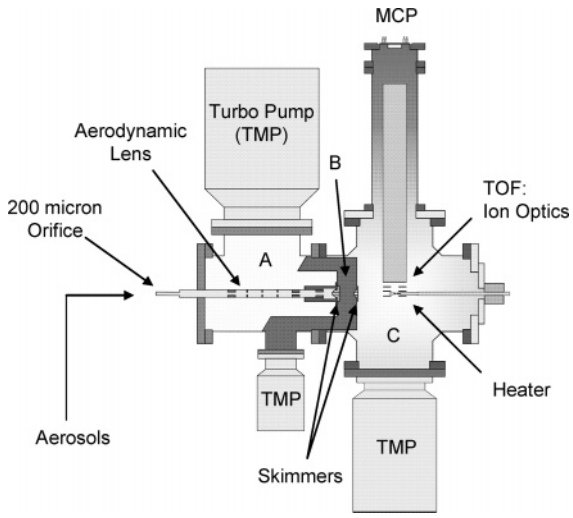

Figure 2. Vacuum-ultraviolet aerosol mass spectrometer (AMS), consisting of three differentially pumped vacuum chambers labeled A, B, and C.

and phenylalanine, the tripeptide phenylalanine−glycine−glycine (phe-gly-gly), and β-carotene. Tryptophan is selected because there is a large body of comparison work that employs a variety of ionization and desorption techniques.[7,8] This report focuses on three unique capabilities of this new method. First, the effect of internal energy on the fragmentation pattern of tryptophan is investigated as a function of both thermal and photoionization energy. Second, the ionization energies of both tryptophan and the tripeptide phe-gly-gly are measured, clearly demonstrating the utility of this technique for obtaining fundamental electronic state properties of amino acids and polypeptide molecules. Finally, we consider the fragmentation-free mass spectra of a large molecule, β-carotene, which can be obtained by carefully adjusting both the method of particle preparation and the temperature of vaporization and photoionization energy.

Experiment Design

Bioaerosols are generated by a constant output atomizer (TSI model no. 3076) using solutions (0.5−1 g/L of H_2O, ethanol, or methanol) of tryptophan, phe-gly-gly, or β-carotene. The liquid droplets are then entrained in a nitrogen carrier gas, preheated to 50 °C, and passed through a room-temperature diffusion dryer to form solid particles. The particle size distribution and number density are measured with a commercial differential mobility analyzer (DMA; TSI model 3081) coupled to a condensation particle counter (CPC; TSI model 3025A). The average particle size can be adjusted by ±20% simply by changing the solution concentration in the atomizer. Tryptophan particles produced in this way exhibit a broad size distribution with a median diameter of 126 nm and a total concentration of 9×10^6 particles/cm^3, as shown in Figure 1.

For time-of-flight (TOF) analysis of biomolecules in the gas phase, the precursor bioaerosols are directed into an aerosol mass spectrometer (AMS) shown in Figure 2. The machine was designed and constructed at the Chemical Dynamics Beamline. Historically, AMSs were designed to measure the chemical composition of tropospheric aerosol particles and are now common tools in both laboratory and field-based instruments.[9−12] The aerosols pass into the vacuum through a 200 μm diameter flow-limiting orifice (4.1 cm^3/s) and then into an aerodynamic lens. The aerodynamic lens consists of five apertures that focus particles into a narrow beam. The lens system used here is nearly identical to the design reported by Zhang et al.[13,14] who compute 80−100% transmission efficiency for particle sizes between 70 and 1000 nm. The particles then exit the lens into a source vacuum chamber (labeled A in Figure 2) pumped by a 2000 L/s turbomolecular pump with an operational base pressure of 5×10^{-2} Pa. The aerosol beam then passes through a 2 mm conical skimmer into a region of differential pumping (B in Figure 2) with an operating pressure of 1×10^{-4} Pa. Finally, the aerosols exit this vacuum chamber through a 4 mm aperture and enter the interaction chamber housing the TOF mass spectrometer. The interaction chamber (C) has an operational pressure of 1×10^{-5} Pa maintained by a 1000 L/s turbo molecular pump.

Once transported into vacuum, the aerosols are thermally vaporized (298−873 K) on a 3 mm diameter heated copper tip inserted between the TOF optics. The expanding gas provides a localized source of biomolecules, which is photoionized by the vacuum-UV photon beam from a synchrotron. The resulting TOF spectrum is detected by a dual chevron multichannel plate (MCP) and recorded on a multichannel scaler with 8 ns bin width. For the TOF spectra reported here, the heater temperatures were selected to ensure complete vaporization of the bioaerosol particles. It has been previously shown that the total ion yield[15] originating from vaporized aerosol particles increases as a function of temperature, reaching a plateau beyond which the ion signal remains nearly constant. This plateau region indicates that the particle undergoes complete vaporization. For the case of tryptophan, the total ion signal, normalized to photon intensity, is observed to be constant within 20% at temperatures exceeding 363 K—indicating complete particle vaporization.

The gas-phase biomolecules produced by particle vaporization undergo single photon ionization (SPI) with tunable VUV light produced by the Advanced Light Source at the Chemical Dynamics Beamline located at Lawrence Berkeley National Laboratory, Berkeley, CA. The beamline, based on an undulator, produces tunable (7−25 eV) VUV radiation at an average photon flux of 1×10^{16} photons/s with a spectral bandwidth of 2.5%. The synchrotron light is passed through an argon gas filter and two MgF_2 windows to remove high-energy harmonics produced by the undulator. The photon beam spot size is ~200 μm in the region where the photon and particle beam intersect. One stage of differential pumping is used to couple the TOF mass spectrometer to the ultrahigh-vacuum environment of the beamline (10^{-7} Pa). Typical photoionization TOF spectra of tryptophan vaporized at 373, 420, and 573 K

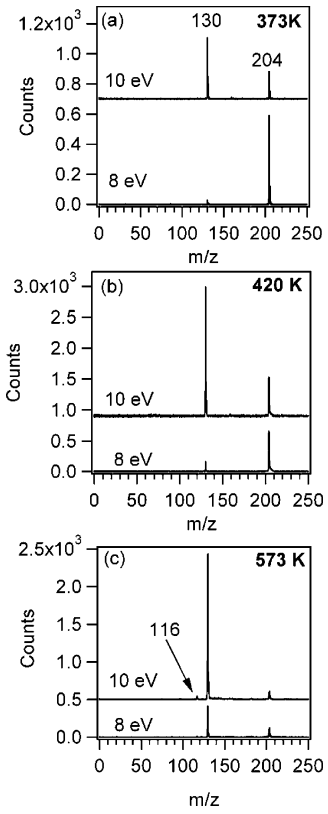

Figure 3. Photoionization mass spectra at 8 and 10 eV of tryptophan obtained by vaporizing bioaerosols at (a) 373 (b) 420, and (c) 573 K.

are shown in Figure 3. Further details regarding beamline specifications have been described elsewhere.[16]

The synchrotron light source is quasi-continuous (500 MHz), while the particle beam is entrained in a continuous flow of N_2 (1 L/min). Therefore, TOF mass spectra are obtained by pulsing the ion optics at 5 kHz. Spectra are obtained by holding both the extractor and repeller plate near the ground and then applying a 100 V, 3 μs pulse to the repeller plate. After leaving the ionization region, the photoions are post-accelerated by a second 10 μs, 1 kV pulse and are then detected on a microchannel plate located at the end of a 1 m flight tube. This pulsing scheme is essential for obtaining high-quality TOF spectra when the heater tip (at ground potential) is positioned between the 7.62 cm diameter repeller and extractor ion optics. In this configuration the synchrotron beam probes 1−5 mm from the end of the heated tip, thereby intersecting the dense part of the vapor expansion. The TOF spectra reported here are obtained by averaging 20 000−100 000 ion pulses requiring only a total acquisition time of 4−10 s/spectra. Replicate TOF spectra obtained in this way and normalized to incoming photon flux are reproducible to within 5−10%. The constant-output atomizer produces a stable stream of particles and functions reliably over the course of an experimental session (12+ hours).

Assuming that the particle vapor originates from a point source, the molecular density of the expanding gas is expected to diminish as $1/r^2$, where r is the distance between the synchrotron beam and the heated tip. Therefore, the ion signal produced at any point in the gas expansion would also decay as $1/r^2$. However, since the synchrotron beam is weakly focused, ions emanate not from a point source in the expanding gas but rather from a "stripe". Under these geometric conditions the ion signal is expected to diminish as $\sim 1/r$. This is illustrated in Figure 4 with glycine particles vaporized at 473 K and

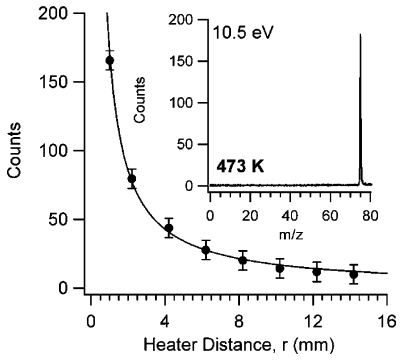

Figure 4. Glycine parent signal ($m/z = 75$) (inset) as a function of distance, r, between the photon beam and heater tip. The solid line is proportional to $1/r$.

photoionized at 10.5 eV. The parent glycine ion signal (Figure 4 inset) decays as expected by $\sim 1/r$. Similar results are obtained for tryptophan. The 10.5 eV photoionization spectrum of glycine reported here consists of a single parent molecular ion peak without fragmentation. This is in contrast to the results of Jochmis et al.,[17] who recently reported a 10.0 eV photoionization spectrum of glycine that is dominated by the smaller $NH_2CH_2^+$ fragment ion ($m/z = 30$). In that study, macroscopic samples of glycine solid were sublimed at 426−473 K to obtain sufficient quantities of gas-phase glycine for photoionization. Since the temperature and photon energy employed in that study are nearly identical to the conditions reported here, the exact origin of this discrepancy is unclear. It may be due to important differences in vaporizing macroscopic vs nanoparticle samples of glycine, instead of fragmentation induced by the incident photon energy as concluded by Jochims et al.[17]

The flux and geometry of the bioparticle beam are characterized in situ. Nanometer-sized particles are invariably charged, which allows the particle flux through the end station to be conveniently measured with a Faraday cup. On average there is 5 pA of particle current, yielding a particle flux of 3×10^7 particles/s through the AMS, assuming on average 1 charge/particle. This assumption appears reasonable given that the magnitude of this signal is consistent with a flux predicted (3.7×10^7 particles/s) using the total particle density (9×10^6 particles/cm^3) measured independently by the DMA-CPC (Figure 1) and the sampling rate (4.1 cm^3/s) of the aerosol mass spectrometer. The total mass density of particles shown in Figure 1, under our conditions, is computed to be 2×10^4 μg/m^3, given that the density of solid tryptophan is 1.34 g/cm^3. From the sampling rate of the AMS, we can estimate that the molar flux of tryptophan entering the interaction region is $\sim$450 pmol/s.

The width of the bioparticle beam was determined by scanning a razor blade through a beam of potassium iodide particles and taking the derivative of the particle current with respect to position. The resulting beam profile, shown in Figure 5, is obtained at the position of the heater tip, located 30.5 cm from the exit of the aerodynamic lens. The full width at half-maximum (fwhm) of the particle beam is determined to be 1.5 mm, indicating that the angular divergence of particles exiting the aerodynamic lens is approximately 0.3°.

Results and Discussion

Tryptophan. There have been many previous photoionization mass spectrometry studies of gas-phase tryptophan.[7,8,17−19] This is due in part to the UV-active chromophore that allows easy ionization with 1 + 1 multiphoton ionization (MPI). The previous works on tryptophan can be broadly distinguished by

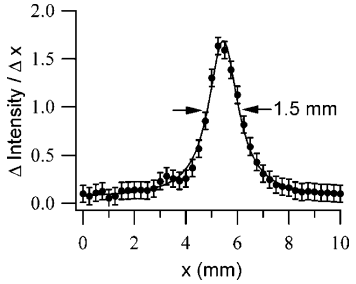

Figure 5. Potassium iodide particle beam profile obtained by scanning a razor blade through the beam and measuring the change in current with a picoammeter. From the derivative of current vs position the particle beam is determined to have a fwhm of 1.5 mm.

both the method of volatilization and ionization. Zhan and coworkers[20] have compiled a table of these various methods. To evaluate the general utility of each technique for the production of fragment-free tryptophan mass spectra, a parent/fragment ratio (*M*/*F*) is reported. *M*/*F* is simply the ratio of the parent molecular ion ($m/z = 204$) intensity to the methylene indole ($m/z = 130$) fragment. The methylene indole ion is the dominant fragmentation channel that appears in nearly every photon or electron impact ionization mass spectrum of tryptophan.[20] As expected, the techniques that couple supersonic jet cooling with laser desorption obtain the highest *M*/*F* ratios, exhibiting a 7−7.5 times enhancement of the molecular parent ions over the fragment ions. Conversely, desorption and ionization without vibrational cooling produce small parent ion signals with *M*/*F* ratios between 0 and 1.[20] It should also be pointed out that the *M*/*F* ratio is somewhat sensitive to both the laser pulse width (femtoseconds vs nanoseconds) and the two photon ionization wavelengths as discussed by Wienkauf et al.[21] However, these differences seem to be of minor importance when compared to jet cooling.

The tryptophan photoionization mass spectra, shown in Figure 3, are obtained by varying both the particle vaporization temperature and the ionization energy. The spectra at 8 and 10 eV measured at a heater temperature of 373 K exhibit two main features. The 8.0 eV spectrum is dominated by a single peak at mass 204— corresponding to the tryptophan molecular ion. The integrated area *M*/*F* ratio at 8.0 eV (373 K), Figure 3a, is determined to be 23, already exceeding the best results recently reported by Puzzi et al.[18] for laser desorption jet cooling MPI mass spectra recorded at a two-photon energy of 9.2 eV. At 10 eV photon energy a second peak appears at mass 130 corresponding to the methylene indole fragment ion ($[C_9H_8N]^+$) produced by the scission of the $C_\alpha-C_\beta$ bond.[20] As discussed above, this fragment ion has been observed in nearly every previous study of tryptophan obtained by a diverse set of vaporization techniques (laser and thermal desorption) combined with many different ionization schemes (femtosecond and nanosecond multiphoton ionization as well as electron impact). Based upon the laser power dependence of this peak ($m/z = 130$), the formation of the methylene indole ion ($m/z = 130$) has been explained by the absorption of an additional photon by the tryptophan molecular ion—consistent with the so-called ladder switching model of multiphoton ionization.[8,20] However, since the spectra shown in Figure 3 are produced, in our case, by SPI, the appearance of $m/z = 130$ at 10 eV can only occur by excess internal energy imparted to the molecular ion during photoionization. This result suggests that the appearance of mass 130 in the MPI spectra could also be partly due to unknown amounts of internal energy imparted into the neutral molecule during the two-photon ionization steps.

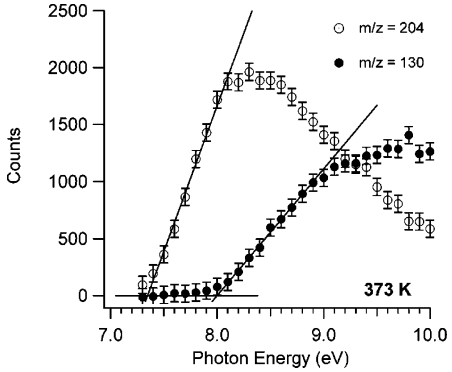

Figure 6. Photoionization efficiency curves at 373 K for the tryptophan parent ion (○) and the methylene indole fragment (●). Also shown is a nonlinear least-squares fit to the photoionization onset used to obtain appearance energies for both ions.

As the vaporization temperature is increased to 420 K, both the 8 and 10 eV photoionization spectra exhibit a pronounced shift in intensity from the tryptophan molecular ion (204) into the methylene indole fragmentation channel (130). As the temperature is further increased to 573 K, the shift becomes more pronounced, with the 8 and 10 eV spectra exhibiting *M*/*F* ratios of 0.6 and 0.1, respectively. At 573 K, a second fragment peak at $m/z = 116$, which is absent in the 373 and 420 K spectra, is detected and assigned to the indole fragment $[C_8H_6N]^+$. This fragment ion has also been observed at high laser fluxes in MPI studies and has been assigned to a direct dissociation of the parent tryptophan ion.[20] This interpretation is consistent with the results presented here, which indicate that the appearance of the 116 fragment is entirely due to the excess internal energy at 573 K in the neutral molecule prior to photoionization.

The particle vaporization VUV photoionization technique described here provides an important complement to MPI studies of fragile biomolecules and can aid in the interpretation of various fragmentation channels. By adjusting both the photon energy and the thermal energy, fragmentation induced by the neutral or ion internal energy can be directly compared with the complex fragmentation channels observed in MPI. Dey and Grotemeyer[8] constructed complex breakdown diagrams of tryptophan that include both multiphoton as well as dissociative ionization channels. The accessibility of these channels is determined by the number of photons required to produce various fragment ions. For example, at low laser fluences the MPI mass spectra are dominated by the tryptophan (204) and methylene indole (130) ions. At very high intensities, the tryptophan ion is completely dissociated into its atomic constituents by sequential photon absorption. In contrast, only two fragments appear in the SPI spectra reported here at moderate vaporization temperatures. The relative fragment population as well as the parent ion intensity can be precisely controlled either by tuning the internal energy of the neutral (by vaporization temperature) or the molecular ion (by photon energy).

The tryptophan photoionization efficiency (PIE) spectrum is obtained by measuring TOF spectra as a function of photon energy. The PIE curves for tryptophan particles vaporized at 373 K are shown in Figure 6. The appearance energy of the tryptophan molecular ion, determined by a nonlinear least-squares fit to the slope of the ionization onset, is determined to be 7.3 ± 0.2 eV. Presently, a more accurate determination has not been made due to the bandwidth of the undulator radiation and the inability to scan the undulator to energies less than 7.2 eV at the 1.9 GeV storage ring operation. Nevertheless, the value reported here is in good agreement with the adiabatic ionization

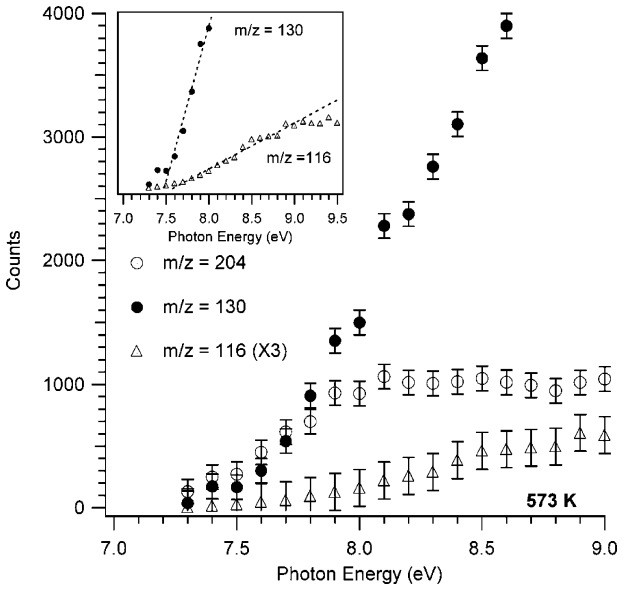

Figure 7. Photoionization efficiency curves at 573 K for the tryptophan parent ion (○), the methylene indole (●) and indole (△) fragments. The inset shows the linear fit to the photoionization onset used to obtain appearance energies for methylene indole and indole fragments.

energy measured via photoelectron spectroscopy reported by Campbell et al.[4] The methylene indole fragment ($m/z = 130$) appears at 8.0 ± 0.1 eV, which is 0.7 eV above the parent molecular ion onset. This value is significantly lower than the 9.2 eV estimate provided by MPI.[8] The $m/z = 204$ signal plateaus around 8.3 eV, while the mass 130 peak intensity monotonically increases as a function of photon energy. This behavior indicates a direct interplay between the photoionization of the tryptophan molecule and dissociation of the tryptophan molecular ion by the additional internal excitation.

To further explore the relationship between internal energy in the molecular ion with that of the neutral precursor, PIE curves were measured at 573 K, as shown in Figure 7. Unfortunately, changes in the appearance energy of the molecular ion cannot be directly ascertained because of the limited photon energy range of the undulator. However, it has been shown before that the excess internal energy has a small influence on the absorption cross-section of the neutral molecule, and therefore any changes in the ionization energy of tryptophan are expected to be small.[22] This has been observed in the photoionization spectra of alkanes reported by Steiner et al.[23] However, there is a dramatic change in the methylene indole fragment (130) appearance energy, which is found to be 7.5 ± 0.1 eV at the 573 K vaporization temperature. This is a 0.5 eV shift from the 8.0 eV threshold measured at 373 K. In addition, as shown in Figure 3, the indole (m/z 116) fragment also appears in the 573 K spectra. The appearance energy of the m/z 116 fragment is also determined to be 7.5 ± 0.1 eV (at 573 K). It is interesting to note that the 116 fragment only appears at 573 K (Figure 3), suggesting that the effect of the internal energy on this fragmentation channel is different from that of the methylene indole ($m/z = 130$). In general, because the amount of internal energy imparted during the photoionization step is likely to be similar at 373 and 573 K, the shift in appearance energy of the methylene indole fragment is primarily due to the additional thermal energy imparted into the neutral tryptophan molecule at the time of vaporization.

The average internal energy of a collection of harmonic oscillators is given by

$$E_{\text{therm}} = \sum_{i=1}^{s} \frac{h\nu_i}{e^{(h\nu/kT)_i} - 1}$$

To compute the average internal energy of a tryptophan molecule as a function of temperature, a set of frequencies ν_i was computed using Gaussian[24] at the B3LYP/6-3111G level of theory. Vibrational analysis was done after full geometry optimization. Over the 350 K temperature range investigated computationally, the average internal energy of a tryptophan molecule changes by ~1 eV, as shown in Figure 8. The change in average internal energy by raising the temperature from 373 to 573 K is 0.62 eV. From inspection of the PIE curves at 373 and 573 K, a change of 0.5 eV in the appearance energy of the 130 fragment is observed. This suggests that nearly 80% of the theoretically computed internal energy can go into dissociating the tryptophan molecular ion into the methylene indole fragment, assuming that the vibrational frequencies of the neutral tryptophan molecule are similar to those of the molecular ion. This direct connection between the internal energy and the appearance energy of the fragments has been pointed out by Chupka[25] in the dissociative photoionization spectra of alkanes recorded by Steiner et al.[23]

To isolate the contribution of internal energy of the neutral tryptophan molecule from the internal energy imparted by photoionization, a series of temperature-dependent spectra were obtained at a fixed photon energy. Figure 9a shows that the *M*/*F* ratio (204/130) at 8.25 eV is an exponentially decreasing function of temperature. Over the 200 K range studied, the *M*/*F* ratio is observed to vary by a factor of 20. This exponential dependence is "Arrenhius-like", suggesting that within the neutral molecule there is a phenomenological activation energy, which when overcome, leads to efficient fragmentation when the thermally activated neutral molecule is photoionized.

The influence of the internal energy on fragmentation can be examined in greater detail by plotting the ratio of mass 204 to 130 as a function of both temperature and photon energy, as shown in Figure 9b. For a fixed temperature, the *M*/*F* ratios monotonically decrease with photon energy as increasing amounts of internal energy are imparted into the tryptophan molecule, thus enhancing dissociative photoionization. In general the *M*/*F* ratios exponentially decrease with temperature over the photon energy range studied and are consistent with the results for 8.25 eV photoionization shown in detail in Figure 9a. As expected, for all temperatures, the highest *M*/*F* ratios are observed for near-threshold (7.9 eV) ionization, where minimal amounts of internal energy result from photoexcitation. Figure 9b also clearly shows that a given *M*/*F* ratio can be obtained by varying two independent parameters: photon energy and vaporization temperature. For example, a *M*/*F* ratio of ~1 can be observed either by threshold ionization at 573 K or by 9.5 eV photoionization at 373 K.

In this way, Figure 9b can yield some insight into the large variation of *M*/*F* ratios (labeled 1−11 in Figure 9b) reported in previous MPI studies of tryptophan. In general, most studies that employ jet cooling (labeled 2, 10, and 6 in Figure 9b) obtain *M*/*F* ratios higher than the values in the 373 K isotherm, indicating good quenching of the thermal energy deposited into the neutral molecule during the initial desorption step. There are, however, a few studies (labeled 1, 3, 4, and 9 in Figure 9b) that use jet cooling yet report lower *M*/*F* ratios, between the 373 and 573 K isotherms. This could suggest incomplete cooling in the molecular beam expansion or additional excitation of internal energy during multiphoton excitation.

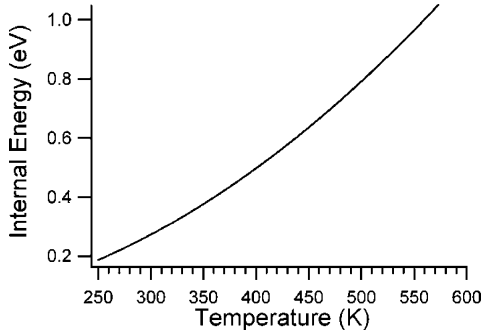

Figure 8. Internal energy of tryptophan vs temperature computed using the vibrational frequencies calculated with Gaussian.[24]

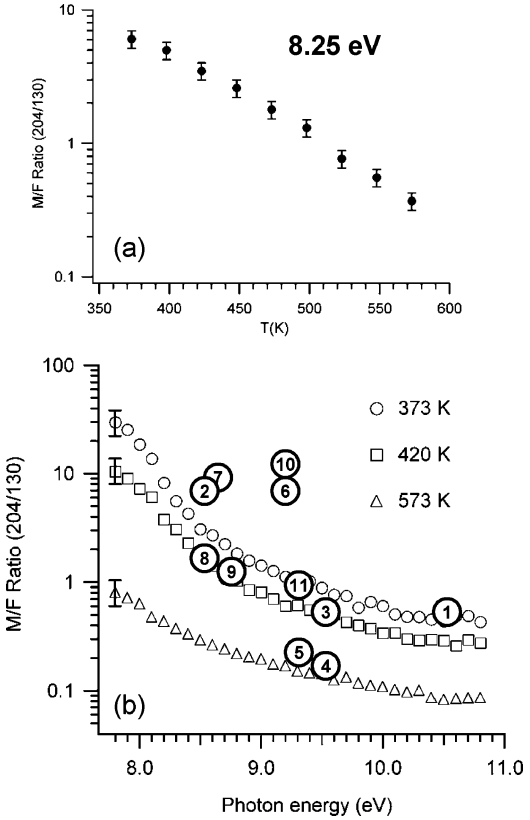

Figure 9. (a) *M*/*F* ratio (204/130) as a function of temperature at a photoionization energy of 8.25 eV. (b) *M*/*F* ratio at 373 (○), 420 (□), and 573 K (△) as a function of photon energy. Also included are *M*/*F* ratios obtained from previous photoionization studies of tryptophan (circled 1−11): (1) Ayre et al.[31] thermal desorption (423 K) + jet cooling; (2) Rizzo et al.[26] thermal desorption (503 K) + jet cooling; (3) Aicher et al.[32] nanosecond photoionization + jet cooling; (4) Aicher et al.[32] femtosecond photoionization + jet cooling; (5) Ayre et al.[31] thermal desorption (423 K); (6) Dey and Grotemeyer[8] infrared laser desorption + jet cooling; (7) Elokhin et al.[33] aqueous cryomatrix; (8) Zhan et al.[20] desorption from stylized glass; (9) Rizzo et al.[7] thermospray (473 K) + jet cooling; (10) Piuzzi et al.[18] laser desorption + jet cooling; (11) Nagra et al.[30] rapid heating + jet cooling.

For example, Rizzo et al.,[26] using a nonresonant two-photon energy of 8.55 eV (2 × 4.28 eV), obtain a *M*/*F* ratio of 7.26.[20] In their experiment, solid tryptophan is introduced into the gas phase using a 500 K thermal desorption cell coupled to a pulsed valve for supersonic jet cooling. From inspection of Figure 9b, the *M*/*F* ratio obtained by Rizzo et al.[26] clearly indicates that tryptophan molecules produced in this way have internal temperatures less than 373 K, thereby confirming that there is efficient quenching of internal degrees of freedom in their molecular beam expansion. This is in contrast to previous work, also conducted by Rizzo et al.,[7] that employed a different thermospray source, volatilizing an aqueous solution to produce gas-phase tryptophan. Despite lower source temperatures (∼473 K), jet cooling, and similar two photon ionization energies (2 × 4.35 eV), a much smaller *M*/*F* ratio of 1.2 was observed. Accordingly, this would suggest that tryptophan molecules produced by the thermospray source remain hot (∼420 K) at the time of photoionization. Given the technical differences in the thermal desorption and thermospray sources employed,[7,26] this is perhaps not surprising.

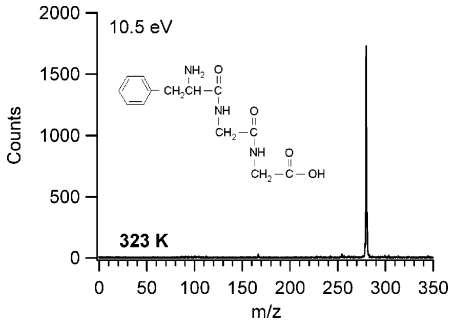

Figure 10. Photoionization mass spectrum at 10.5 eV of phe-gly-gly obtained from nanoparticles vaporized at 323 K.

It has been shown above that by using a particle beam of tryptophan, the appearance of the photoionization mass spectrum can been manipulated by tuning the internal energy of either the precursor neutral molecule or the photoionization energy. This is of great utility in determining how internal energy couples to fragmentation, as is shown for the case of tryptophan. From a more practical viewpoint, the general applicability of using nanoparticles to introduce fragile biomolecules into the gas phase is tested with more complex molecules, including polypeptides. As will be shown below, "fragmentation-free" mass spectra can be obtained for the tripeptide phe-gly-gly. This allows the accurate determination of the ionization energy of this molecule for the first time.

Phenylalanine−Glycine−Glycine and β-Carotene. Solid nanometer-sized phe-gly-gly particles were made by first dissolving 0.5 g of the polypeptide in 0.5 L of methanol. As with tryptophan, the solution was atomized and dried, yielding a distribution of solid nanoparticles similar to that shown in Figure 1. The particles were focused onto the heater, maintained at a temperature of 323 K. It should be pointed out that TOF photoionization mass spectra of phe-gly-gly could not be obtained by preparing particles from a pure water solution. The resulting 10.5 eV photoionization mass spectrum of phe-gly-gly is shown in Figure 10. The spectrum is dominated by a single peak at $m/z = 279$ (the phe-gly-gly molecular ion) with a signal-to-noise ratio of ∼800. The acquisition time for the spectra shown in Figure 10 is approximately 10 s, corresponding to the introduction of approximately ∼1 nmol of material into the photoionization region.

In separate experiments, the PIE curves for phe-gly-gly, glycine, and phenylalanine are shown in Figure 11. The ionization energy of phe-gly-gly is determined to be 9.1 ± 0.1 eV, very similar to the threshold measured for glycine, which is 9.3 ± 0.1 eV ($T = 573$ K), but 0.5 eV higher than the appearance energy of phenylalanine, 8.6 ± 0.1 eV ($T = 523$ K), as is also shown in Figure 11. To our knowledge, this is the first reported ionization energy for phe-gly-gly. Using particle vaporization with SPI, a more systematic study of how the ionization energy evolves as a function of peptide linkage and length in glycine, glycine−glycine, phe-gly-gly, phe-gly-

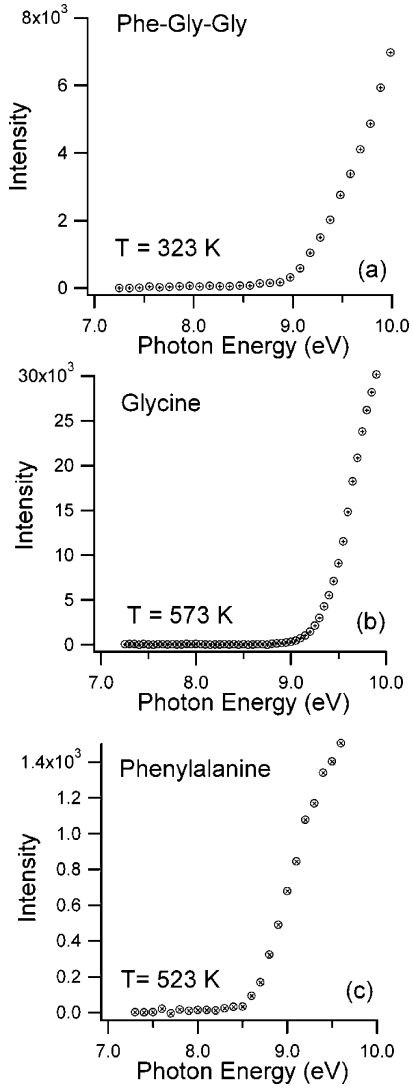

Figure 11. Photoionization efficiency curves of (a) phe-gly-gly, (b) glycine, and (c) phenylalanine obtained at vaporization temperatures of 323, 573, and 523 K, respectively.

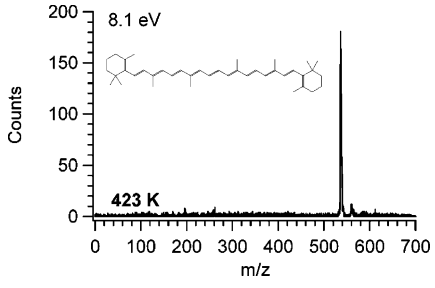

Figure 12. Photoionization mass spectrum at 8.1 eV of β-carotene obtained at a heater temperature of 423 K.

gly-phe, is being undertaken and will be the subject of a forthcoming publication.

β-Carotene nanoparticles were prepared by dissolving 0.5 g/L of sample in a 50:50 methanol/water solution. The solution was kept in the dark during the experiment to avoid the possibility of photodegradation. The resulting particle size distribution produced by the atomizer is similar to that shown in Figure 1. The 8.1 eV photoionization spectrum of β-carotene generated by particles vaporized at 423 K is shown in Figure 12. Once again the spectrum is dominated by a single peak corresponding to the parent molecular ion ($m/z = 536.9$) with a signal-to-noise ratio of 50−100. The spectrum shown in Figure 12 is very similar to the MPI mass spectrum reported by Dey et al.[27] on jet-cooled β-carotene. However, there are large differences in the experimental conditions. In that study, β-carotene was introduced into the gas phase via CO_2 laser desorption and cooled in a molecular beam expansion. Dey et al.[27] estimated that the resulting vibrational temperature of β-carotene in the expansion was 100 K. For the experiments reported here, this may suggest that there could be some quenching of internal energy within the expanding gas cloud after nanoparticle vaporization. Some evidence for such cooling was reported by Woods et al.[28] in the translational energy distribution of vapor molecules emanating from laser-vaporized ethylene glycol particles. Unfortunately, the magnitude of such vibrational cooling cannot be directly ascertained in the experiments reported here.

The nanoparticle source described here clearly affords a number of advantages over conventional thermal and laser desorption methods for obtaining fragment-free photoionization mass spectra. We postulate that there are at least three main reasons for this. First, the nanoparticle beam is substrate-free, removing the need to supply additional thermal energy to break intermolecular biomolecule−substrate bonds. In fact, it has been shown in a number of studies[20,29] that substrate effects (e.g. Teflon vs glass) in desorption experiments can exert considerable influence on the amount of fragmentation produced in a photoionization mass spectrum.

Second, nanometer-sized bioaerosol particles undoubtedly undergo very rapid heating during the short residence times on the heated tip. Nagra et al.[30] showed that heating rates of 10^6-10^8 K/s followed by supersonic jet cooling produced a 9.3 eV MPI spectrum of tryptophan with a M/F ratio of ~1. This is very similar to the M/F ratio observed in the 9.3 eV SPI mass spectrum of tryptophan nanoparticles vaporized at 373 K reported here and shown in Figure 9b.

Last, there is some evidence that the nanoparticle morphology (e.g. intermolecular bonding) may play a role in the thermal release of intact biomolecules into the gas phase. Specifically, phe-gly-gly photoionization mass spectra could only be obtained by aerosolizing solutions prepared in methanol. This suggests that more polar solvents, like water, increase the amount of intra- and intermolecular hydrogen bonding in the nanoparticle and consequently increase the thermal energy needed to liberate the intact tripeptide molecule. Further experiments are planned to examine how nanoparticle morphology (e.g. nanocrystals vs loose aggregates) influence the production of intact, neutral gas-phase biomolecules.

Conclusions

Using nanoparticle vaporization as a source of gas-phase biomolecules affords a number of advantages as described above. First, vaporizing small nanoparticles composed of biomolecules in a vacuum appears to reduce the amount of decomposition that generally occurs in pyrolysis in the presence of air. Second, given the superior signal-to-noise ratio and intensity of the parent ion in these photoionization mass spectra, the complex experimental arrangement required to jet-cool laser-desorbed molecules can be eliminated. Third, the amount of thermal internal energy can be precisely controlled to adjust the relative populations of fragment ions. This ability not only affords greater insight into how internal energy affects fragmentation but is also another way to "sequence" large polypeptides and perhaps proteins. Finally, further improvements can be made to the atomizer to introduce smaller quantities of valuable biological nanoparticles, thereby improving the analytical utility and sensitivity of this technique.

Acknowledgment. The authors wish to acknowledge Dr. Jinian Shu of the Chemical Dynamics Beamline for the design and construction of the AMS. We also thank Darcy Peterka for valuable scientific discussions. M.A. acknowledges support from the Laboratory Directed Research and Development (LDRD) program at LBNL. This work was supported by the Director, Office of Energy Research, Office of Basic Energy Sciences, Chemical Sciences Division of the U.S. Department of Energy under Contract No. DE-AC02-05CH11231.

References and Notes

(1) Tanaka, K. *Angew. Chem., Int. Ed.* **2003**, *42*, 3860.

(2) Reinders, J.; Lewandrowski, U.; Moebius, J.; Wagner, Y.; Sickmann, A. *Proteomics* **2004**, *4*, 3686.

(3) Weinkauf, R.; Schermann, J. P.; de Vries, M. S.; Kleinermanns, K. *Eur. Phys. J. D* **2002**, *20*, 309.

(4) Campbell, S.; Beauchamp, J. L.; Rempe, M.; Lichtenberger, D. L. *Int. J. Mass. Spectrom. Ion. Processes* **1992**, *117*, 83.

(5) Nir, E.; Janzen, C.; Imhof, P.; Kleinermanns, K.; de Vries, M. S. *J. Chem. Phys.* **2001**, *115*, 4604.

(6) Vekey, K. *J. Mass Spectrom.* **1996**, *31*, 445.

(7) Rizzo, T. R.; Park, Y. D.; Levy, D. H. *J. Am. Chem. Soc.* **1985**, *107*, 277.

(8) Dey, M.; Grotemeyer, J. *Org. Mass Spectrom.* **1994**, *29*, 659.

(9) Jayne, J. T.; Leard, D. C.; Zhang, X. F.; Davidovits, P.; Smith, K. A.; Kolb, C. E.; Worsnop, D. R. *Aerosol Sci. Technol.* **2000**, *33*, 49.

(10) Noble, C. A.; Prather, K. A. *Mass Spectrom. Rev.* **2000**, *19*, 248.

(11) Suess, D. T.; Prather, K. A. *Chem. Rev.* **1999**, *99*, 3007.

(12) Nash, D. G.; Liu, X. F.; Mysak, E. R.; Baer, T. *Int. J. Mass Spectrom.* **2005**, *241*, 89.

(13) Zhang, X. F.; Smith, K. A.; Worsnop, D. R.; Jimenez, J.; Jayne, J. T.; Kolb, C. E. *Aerosol Sci. Technol.* **2002**, *36*, 617.

(14) Zhang, X. F.; Smith, K. A.; Worsnop, D. R.; Jimenez, J. L.; Jayne, J. T.; Kolb, C. E.; Morris, J.; Davidovits, P. *Aerosol Sci. Technol.* **2004**, *38*, 619.

(15) Mysak, E. R.; Wilson, K. R.; Jimenez-Cruz, M.; Ahmed, M.; Baer, T. *Anal. Chem.* **2005**, *77*, 5953.

(16) Heimann, P. A.; Koike, M.; Hsu, C. W.; Blank, D.; Yang, X. M.; Suits, A. G.; Lee, Y. T.; Evans, M.; Ng, C.; Flaim, C.; Padmore, H. A. *Rev. Sci. Instrum.* **1997**, *68*, 1945.

(17) Jochims, H. W.; Schwell, M.; Chotin, J. L.; Clemino, M.; Dulieu, F.; Baumgartel, H.; Leach, S. *Chem. Phys.* **2004**, *298*, 279.

(18) Piuzzi, F.; Dimicoli, I.; Mons, M.; Tardivel, B.; Zhao, Q. C. *Chem. Phys. Lett.* **2000**, *320*, 282.

(19) Grotemeyer, J.; Schlag, E. W. *Acc. Chem. Res.* **1989**, *22*, 399.

(20) Zhan, Q.; Wright, S. J.; Zenobi, R. *J. Am. Soc. Mass Spectrom.* **1997**, *8*, 525.

(21) Weinkauf, R.; Aicher, P.; Wesley, G.; Grotemeyer, J.; Schlag, E. W. *J. Phys. Chem.* **1994**, *98*, 8381.

(22) Genuit, W.; Nibbering, N. M. M. *Int. J. Mass. Spectrom. Ion. Processes* **1986**, *73*, 61.

(23) Steiner, B.; Giese, C. F.; Inghram, M. G. *J. Chem. Phys.* **1961**, *34*, 189.

(24) Frisch, M. J.; Trucks, G. W.; Schlegel, H. B.; Scuseria, G. E.; Robb, M. A.; Cheeseman, J. R.; Zakrzewski, V. G.; Montgomery, J. A., Jr.; Stratmann, R. E.; Burant, J. C.; Dapprich, S.; Millam, J. M.; Daniels, A. D.; Kudin, K. N.; Strain, M. C.; Farkas, O.; Tomasi, J.; Barone, V.; Cossi, M.; Cammi, R.; Mennucci, B.; Pomelli, C.; Adamo, C.; Clifford, S.; Ochterski, J.; Petersson, G. A.; Ayala, P. Y.; Cui, Q.; Morokuma, K.; Salvador, P.; Dannenberg, J. J.; Malick, D. K.; Rabuck, A. D.; Raghavachari, K.; Foresman, J. B.; Cioslowski, J.; Ortiz, J. V.; Baboul, A. G.; Stefanov, B. B.; Liu, G.; Liashenko, A.; Piskorz, P.; Komaromi, I.; Gomperts, R.; Martin, R. L.; Fox, D. J.; Keith, T.; Al-Laham, M. A.; Peng, C. Y.; Nanayakkara, A.; Challacombe, M.; Gill, P. M. W.; Johnson, B.; Chen, W.; Wong, M. W.; Andres, J. L.; Gonzalez, C.; Head-Gordon, M.; S., R. E.; Pople, J. A. *Gaussian 98*, Revision A.7 ed.; Gaussian, Inc.: Pittsburgh, PA, 2001.

(25) Chupka, W. A. *J. Chem. Phys.* **1971**, *54*, 1936.

(26) Rizzo, T. R.; Park, Y. D.; Peteanu, L. A.; Levy, D. H. *J. Chem. Phys.* **1986**, *84*, 2534.

(27) Dey, M.; Moritz, F.; Atkinson, G. H.; Grotemeyer, J.; Schlag, E. W. *J. Chem. Phys.* **1991**, *95*, 4584.

(28) Woods, E.; Miller, R. E.; Baer, T. *J. Phys. Chem. A* **2003**, *107*, 2119.

(29) Beuhler, R. J.; Flanigan, E. O.; Greene, L. J.; Friedman, L. *Biochem. Biophys. Res. Commun.* **1972**, *46*, 1082.

(30) Nagra, D. S.; Zhang, J. Y.; Li, L. *Anal. Chem.* **1991**, *63*, 2188.

(31) Ayre, C. H.; Moro, L.; Becker, C. H. *Anal. Chem.* **1994**, *66*, 1610.

(32) Aicher, K. P.; Wilhelm, U.; Grotemeyer, J. *J. Am. Soc. Mass Spectrom.* **1995**, *6*, 1059.

(33) Elokhin, V. A.; Krutchinsky, A. N.; Ryabov, S. E. *Rapid Commun. Mass Spectrom.* **1991**, *5*, 257.